

## New glass ceramics: an effective conjunction of wet chemistry synthesis and sintering

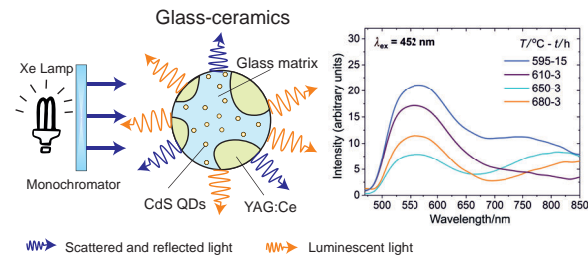
Julia V. Kuznetsova,<sup>\*a</sup> Victoria D. Putilova<sup>b</sup> and Ivan D. Popov<sup>a</sup>

<sup>a</sup> Institute of Solid State Chemistry, Ural Branch of the Russian Academy of Sciences, 620990 Ekaterinburg, Russian Federation. E-mail: jukuznetsova@mail.ru

<sup>b</sup> Institute of Physics and Technology, Ural Federal University, 620002 Ekaterinburg, Russian Federation

DOI: 10.1016/j.mencom.2023.01.041

A glass with CdS nanoparticles was used simultaneously as a matrix for Ce-doped garnet and a yellow-red phosphor to prepare luminescent glass ceramics for the sources of white light. CdS nanoparticles compensate for the unbalanced Ce<sup>3+</sup> emission spectrum of the composite material due to the addition of a red component. The synthesized composite material can be a tunable light converter due to altered luminescence spectra by changing the sintering conditions and excitation wavelength.



**Keywords:** luminescent glass ceramics, alkali silicate glass, YAG:Ce, CdS quantum dots, white light sources.

Currently, highly efficient light sources are in huge demand.<sup>1</sup> Art workshops, museums, printing, medicine, automobile, and aviation industry take the highest requirements on lighting devices: extreme working conditions, high luminous flux, and high color rendering index (CRI). Commercial white LED devices imitating sunlight are mainly based on yttrium aluminum garnet doped by Ce<sup>3+</sup> (YAG:Ce) as a yellow phosphor.<sup>2</sup> It demonstrates high photoluminescence efficiency and maximum intensity at 530–570 nm. However, the white light sources based on this material have disadvantages such as a low CRI and a high correlated color temperature due to the lack of red component in the spectrum. This problem can be solved by the addition of a red phosphor.<sup>3–5</sup> The purpose of this study was to create a new composite material for white light sources with improved efficiency and CRI based on cerium-doped yttrium aluminum garnet and silicate glass with cadmium sulfide quantum dots (CdS QDs).

At the first stage, powdered Ce-doped yttrium-based garnet Y<sub>2.95</sub>Al<sub>5</sub>O<sub>12</sub>:Ce<sub>0.05</sub> was synthesized by a coprecipitation method.<sup>6,7</sup> The stock solution of mother salts was made by dissolving aluminum, yttrium and cerium nitrates in distilled water. This multication (MC) solution was prepared according to a stoichiometric proportion of Y<sub>2.95</sub>Al<sub>5</sub>O<sub>12</sub>:Ce<sub>0.05</sub>, and the total cation concentration was 0.24 mol dm<sup>-3</sup>. Chemical precipitation was performed by the dropwise addition of the MC solution at a rate of 0.6 ml min<sup>-1</sup> to a 1.5 M solution of ammonium bicarbonate with stirring at room temperature. The resulting suspension was

additionally stirred for 30 min and aged at 80 °C for 4 h. Then, it was filtered, and the solid was washed five times with deionized water, rinsed twice with ethanol, and dried at 120 °C for 12 h. After drying, the precursor powder was grinded in an agate mortar and annealed at 500 °C for 2 h in air. Then, the powder was additionally calcined at 900, 1100, 1300, and 1500 °C for 2 h in air. At the second step, the powders of YAG:Ce and glass<sup>†</sup> with dissolved cadmium and sulfur ions were mixed rigorously in an agate mortar for 10 min and compacted into 5 × 2 mm pills. A glass/phosphor weight ratio of 8/1 was used based on the previous results.<sup>8</sup> Further, the pills were sintered in YAG/CdS glass ceramics in air at 610, 650, and 680 °C for 3 h and at 595 °C for 15 h. During the sintering, the glass powder softened and filled voids and pores between the crystalline garnet particles in the initial pill. At the same time, the sintering of ceramics was combined with the growth of cadmium sulfide quantum dots (CdS QDs) in the glass matrix due to the diffusion activation of Cd and S ions at sintering temperatures. Thus, the final composite was a dense ceramics with a homogeneous distribution of crystal and glass phases.

Figure 1 shows the XRD patterns<sup>‡</sup> of YAG:Ce. The initial powder was amorphous until 900 °C. The powder was crystallized at 900 °C when calcination was observed. The size of coherent scattering region (CSR) was around 22 nm. Above 900 °C, peak

<sup>†</sup> Phase identification was performed by X-ray diffraction (XRD) analysis on a Shimadzu diffractometer using CuK $\alpha$  radiation in the range  $2\theta = 10\text{--}80^\circ$  and the Rietveld method. The crystallite size of YAG:Ce powder was calculated by the Williamson–Hall method using the Scherrer equation. The instrumental parameters of broadening were determined using LaB<sub>6</sub> (NIST 660c), which is intended for the calibration of peak positions and shapes. The Ce atom population was calculated using the GSAS software package<sup>17,18</sup> from XRD patterns obtained on a STADI-P (STOE) diffractometer equipped with a linear position-sensitive detector. Polycrystalline silicon with the cell parameter  $a = 5.43075(5)$  Å was used as an external standard.

<sup>‡</sup> The starting materials for YAG-based phosphor were analytical-grade rare earth nitrates Y(NO<sub>3</sub>)<sub>3</sub>·4H<sub>2</sub>O (99.99%), Ce(NO<sub>3</sub>)<sub>3</sub>·6H<sub>2</sub>O (99.99%), Al(NO<sub>3</sub>)<sub>3</sub>·9H<sub>2</sub>O (98%) and ammonium bicarbonate NH<sub>4</sub>HCO<sub>3</sub> from Sigma-Aldrich, which were used without further purification. The SiO<sub>2</sub>–ZnO–Na<sub>2</sub>O–K<sub>2</sub>O–B<sub>2</sub>O<sub>3</sub> glass with Cd and S ions was synthesized and studied earlier.<sup>9–11</sup> The initial concentration of Cd and S during the glass synthesis was about 1 wt%.

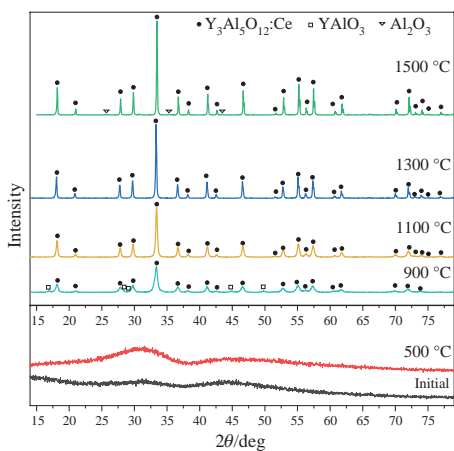


**Figure 1** XRD patterns of YAG:Ce powders calcined at different temperatures. The diffraction peaks were attributed to the cubic garnet structure of  $\text{Y}_3\text{Al}_5\text{O}_{12}:\text{Ce}^{3+}$ . The formation of phases of  $\text{YAlO}_3$  (11.6 wt%) and  $\text{Al}_2\text{O}_3$  (2.6 wt%) was observed at 900 and 1500 °C, respectively.

shapes indicated the growth of crystal particles in the powder as the temperature increased. Thus, the CSR of particles was around 70 nm at 1100 °C. The calculation of CSRs in the samples calcined at 1300 °C and higher failed due to the limits of the Williamson–Hall method. Obtained powder was attributed to pure cubic garnet structure (ICSD 196286<sup>12</sup>) with the cell parameter  $a = 12.0161(1)$ , and the Ce atom population was  $1.90 \pm 0.05\%$  on a basis of Y atoms. Thus, the experimental composition of the synthesized YAG:Ce corresponds to the stoichiometric formula  $\text{Y}_{2.943}\text{Al}_5\text{O}_{12}:\text{Ce}_{0.057}$ . The formation of an intermediate phase of orthorhombic perovskite structure  $\text{YAlO}_3$  with a concentration of 11.6 wt% was observed in the sample annealed at 900 °C, which disappeared at higher temperatures. Additionally, the calcination at 1500 °C led to the formation of an  $\text{Al}_2\text{O}_3$  phase (2.6 wt%).

Figure 2 shows the excitation and emission spectra<sup>8</sup> of YAG:Ce phosphor sintered at different temperatures. Two excitation bands at 344 and 452 nm were attributed to electron transition from the ground state of  $\text{Ce}^{3+}$  ( $2\text{F}_{5/2}, 2\text{F}_{7/2}$ )<sup>13–16</sup> to different crystal field splitting components of the excited 5d state. An increase in the intensity of PL resulted from the enhancement of crystallization degree with heat treatment temperature and a decrease of surface defects.<sup>6,13,15</sup> In comparison with published data,<sup>6</sup> the PL increased without changes in the position of a maximum [Figure 2(b), insert] that indicates the effectiveness of suggested modification method. In particular, a lower rate of dropping the MC solution and a higher ageing temperature allowed us to increase the cation homogeneity during the precipitation. Additionally, the calcination was performed with slow heating and cooling at rates of 300 °C h<sup>−1</sup>. This led to better crystallinity and order of atomic structure of YAG:Ce.

The sample of YAG:Ce powder with the highest PL intensity was used for the synthesis of glass ceramics based on CdS QDs. The CdS QDs in the glass matrix had a wide PL band in a range from 400 to 1100 nm with a maximum at 600–800 nm at room temperatures depending on the heat treatment conditions.<sup>10,11</sup> Typically, the PL of CdS QDs is represented by the interband transition or exciton annihilation mechanism. However, CdS QDs provide a broad luminescence band attributed to the dominance of donor–acceptor pair transitions due to defects in the atomic structure (trap states).<sup>19–21</sup> Nevertheless, such

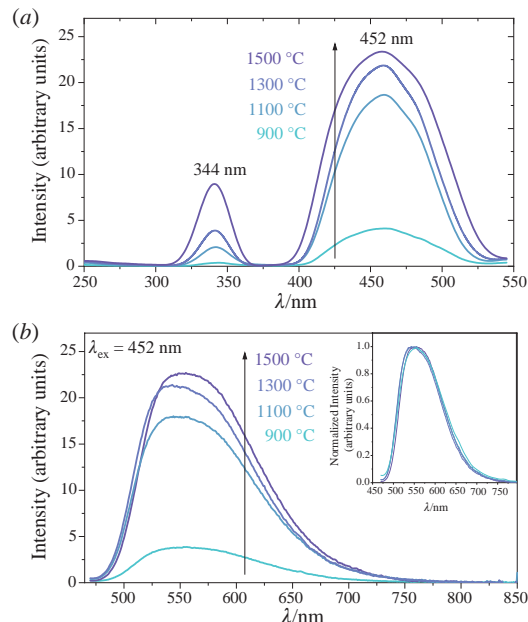


**Figure 2** Photoluminescence (a) excitation and (b) emission of a YAG:Ce phosphor sintered at different temperatures.

luminescence can be tuned because the set and position of defect levels can be controlled by the QD size, which depends on the heat treatment of the used glass.<sup>10,11</sup> Thus, the sintering temperatures used for the synthesis lead to the growth of CdS QDs to 2–4 nm in diameter.<sup>11</sup>

An increase in the sintering temperature led to the formation and intense growth of CdS QDs, which caused the appearance of red components in the spectrum (Figure 3). The CdS QD PL band red shifted and increased with the growth of nanoparticles in the glass matrix during the sintering.<sup>11</sup>

The excitation wavelength demonstrated a significant effect on the shape and position of PL spectra due to partial overlapping of the absorption ranges of garnet phosphors and CdS QDs. The chromaticity coordinates of the resulting glass-ceramic material also depend on the excitation wavelength and the ceramics sintering conditions (Figure 4). The appearance of CdS QDs shifts the color coordinates to the red region due to the enrichment of the spectrum from 650–850 nm. Thus, this method can be

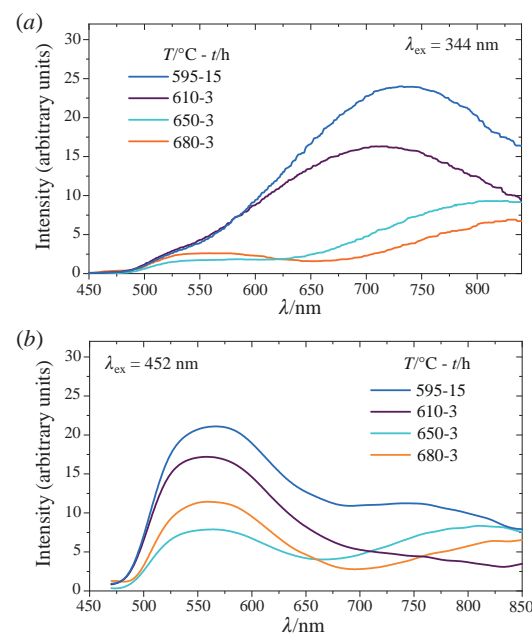


**Figure 3** Photoluminescence of YAG/CdS glass ceramics sintered under different conditions: excitation at (a) 344 and (b) 452 nm. The temperature ( $T/^\circ\text{C}$ ) and duration ( $t/\text{h}$ ) of sintering of YAG/CdS glass ceramics are specified.

<sup>8</sup> Diffuse reflectance and photoluminescence (PL) spectra were recorded on an FS-5 spectrophotometer (Edinburgh Instruments), which was equipped with a Xe lamp, an integrating sphere coated by optical PTFE, a photomultiplier, and an InGaAs detector, in the UV, visible and NIR ranges at ambient temperature.

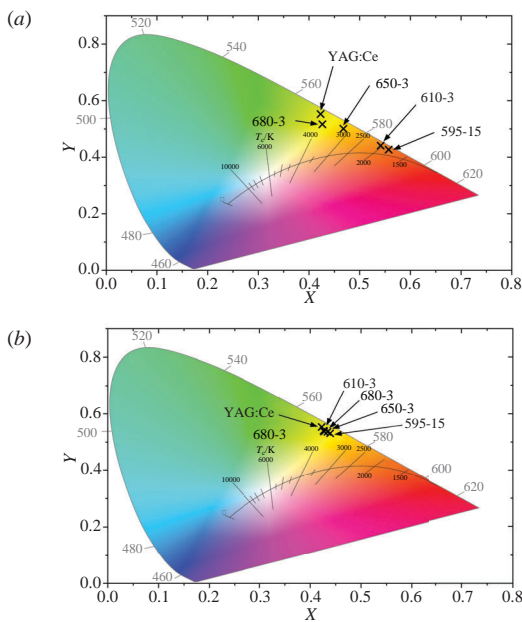


**Figure 4** Chromaticity coordinates of initial YAG:Ce (1500 °C) and YAG/CdS glass ceramics sintered under different conditions: excitation at (a) 344 and (b) 452 nm. The temperature–time of the sintering of YAG/CdS glass ceramics samples is specified.

used to obtain phosphors with different spectral characteristics and change their color by varying the composition, annealing temperature, and excitation wavelengths.

Thus, we obtained a new luminescent composite material based on cerium-doped yttrium aluminum garnet and silicate glass doped with CdS QDs. YAG:Ce powders were produced by coprecipitation from a mixed solution of aluminum, yttrium, and cerium nitrates using ammonium bicarbonate as a precipitant. Glass with CdS QDs simultaneously performs two functions. First, it serves as a matrix that binds the crystalline phase of garnet structured phosphor. This can increase the thermal conductivity and resistance to high light fluxes. Second, the glass with CdS QDs compensates for the unbalanced Ce<sup>3+</sup> emission spectrum due to the appearance of a red component in the emission spectrum of the composite material.

The work was supported by the Russian Science Foundation (Agreement no. 21-72-00060).

## References

- 1 G. B. Nair and S. J. Dhoble, *The Fundamentals and Applications of Light-Emitting Diodes: The Revolution in the Lighting Industry*, Woodhead Publishing, 2021, pp. 155–176.
- 2 Z. Wu and Z. Xia, in *Nitride Semiconductor Light-Emitting Diodes (LEDs): Materials, Technologies, and Applications*, 2<sup>nd</sup> edn., Elsevier, 2018, pp. 123–208.
- 3 Y. Q. Li, N. Hirosaki, R. J. Xie, T. Takeda and M. Mitomo, *Chem. Mater.*, 2008, **20**, 6704.
- 4 M. N. Brekhovskikh, S. Kh. Batygov, L. V. Moiseeva, M. V. Mastryukov and K. S. Nikonov, *Mendeleev Commun.*, 2021, **31**, 887.
- 5 O. A. Lipina, L. L. Surat, A. Yu. Chufarov, A. P. Tyutyunnik and V. G. Zubkov, *Mendeleev Commun.*, 2021, **31**, 113.
- 6 K. Zhang, H.-Z. Liu, Y.-T. Wu and W.-B. Hu, *J. Alloys Compd.*, 2008, **453**, 265.
- 7 S. Sakirzanovas, L. Sun, C. Yan and A. Kareiva, *Mendeleev Commun.*, 2008, **18**, 251.
- 8 Y. V. Kuznetsova and I. D. Popov, *Ceram. Int.*, 2022, **48**, 18972.
- 9 Y. V. Kuznetsova, A. A. Rempel, M. Meyer, V. Pipich, S. Gerth and A. Magerl, *J. Cryst. Growth*, 2016, **447**, 13.
- 10 I. D. Popov, Y. V. Kuznetsova, S. V. Rempel and A. A. Rempel, *J. Nanopart. Res.*, 2018, **20**, 78.
- 11 I. D. Popov, B. Sochor, B. Schummer, Yu. V. Kuznetsova, S. V. Rempel, S. Gerth and A. A. Rempel, *J. Non-Cryst. Solids*, 2020, **529**, 119781.
- 12 V. V. Atuchin, N. F. Beisel, E. N. Galashov, E. M. Mandrik, M. S. Molokeev, A. P. Yelisseyev, A. A. Yusuf and Z. Xia, *ACS Appl. Mater. Interfaces*, 2015, **7**, 26235.
- 13 L. Guerbous and A. Boukerika, *J. Nanomater.*, 2015, 617130.
- 14 A. Lupei, V. Lupei, C. Gheorghe, S. Hau and A. Ikesue, *Opt. Mater. (Amsterdam, Neth.)*, 2014, **37**, 727.
- 15 G. Singh, V. Thomas, V. S. Tiwari and A. K. Karnal, *Ceram. Int.*, 2017, **43**, 9032.
- 16 A. V. Vishnyakov, E. A. Vishnyakova, T. Yu. Kiseleva and I. V. Ivanov, *Mendeleev Commun.*, 2015, **25**, 299.
- 17 A. C. Larson and R. B. Von Dreele, *General Structure Analysis System (GSAS)*, Los Alamos National Laboratory Report LAUR 86-748, 2004.
- 18 B. H. Toby, *J. Appl. Crystallogr.*, 2001, **34**, 210.
- 19 J. J. Ramsden and M. Grätzel, *J. Chem. Soc., Faraday Trans. 1*, 1984, **80**, 919.
- 20 A. Veamatahau, B. Jiang, T. Seifert, S. Makuta, K. Latham, M. Kanehara, T. Teranishi and Y. Tachibana, *Phys. Chem. Chem. Phys.*, 2015, **17**, 2850.
- 21 X. S. Zhao, J. Schroeder, P. D. Persans and T. G. Bilodeau, *Phys. Rev. B*, 1991, **43**, 12589.

Received: 12th July 2022; Com. 22/6956